Hybrid CCTA/SPECT myocardial perfusion imaging findings in patients with anomalous origin of coronary arteries from the opposite sinus and suspected concomitant coronary artery disease

Christoph Gräni, MD,[a] Dominik C. Benz, MD,[a] Christian Schmied, MD,[b] Jan Vontobel, MD,[a] Fran Mikulicic, MD,[a] Mathias Possner, MD,[a] Olivier F. Clerc, MD,[a] Julia Stehli, MD,[a] Tobias A. Fuchs, MD,[a] Aju P. Pazhenkottil, MD,[a] Oliver Gaemperli, MD,[a,b] Ronny R. Buechel, MD,[a] and Philipp A. Kaufmann, MD[a]

[a] Department of Nuclear Medicine, Cardiac Imaging, University Hospital Zurich, Zurich, Switzerland
[b] Department of Cardiology, University Hospital Zurich, Zurich, Switzerland

Received Oct 8, 2015; accepted Nov 5, 2015
doi:10.1007/s12350-015-0342-x

Background. **Anomalous coronary arteries originating from the opposite sinus of Valsalva (ACAOS) are associated with adverse cardiac events. Discrimination between ACAOS and coronary artery disease (CAD)-related perfusion defects may be difficult. The aim of the present study was to investigate the value of hybrid coronary computed tomography angiography (CCTA)/SPECT-MPI in patients with ACAOS and possible concomitant CAD.**

Methods. **We retrospectively identified 46 patients (mean age 56 ± 12 years) with ACAOS revealed by CCTA who underwent additional SPECT-MPI. ACAOS with an interarterial course were classified as malignant, whereas all other variants were considered benign. CCTA/SPECT-MPI hybrid imaging findings (ischemia or scar) were analyzed according to the territory subtended by an anomalous vessel or a stenotic coronary artery.**

Results. **Twenty-six (57%) patients presented with malignant ACAOS. Myocardial ischemia or scar was found only in patients who had concomitant obstructive CAD in the vessel matching the perfusion defect as evidenced by hybrid CCTA/SPECT imaging.**

Conclusion. **Hybrid CCTA/SPECT-MPI represents a valuable non-invasive tool to discriminate the impact of ACAOS from concomitant CAD on myocardial ischemia. Our results suggest that in a middle-aged population myocardial ischemia due to ACAOS per se may be exceedingly rare and is more likely attributable to concomitant CAD. (J Nucl Cardiol 2017;24:226–34.)**

Key Words: Hybrid • CCTA • SPECT • anomalous coronary arteries originating from the opposite sinus of Valsalva • ACAOS

See related editorial, pp. 235–238

Christoph Gräni and Dominik C. Benz share first authorship.
Ronny R. Buechel and Philipp A. Kaufmann share last authorship.
Reprint requests: Philipp A. Kaufmann, MD, Department of Nuclear Medicine, Cardiac Imaging, University Hospital Zurich, Ramistrasse 100, 8091 Zurich, Switzerland; *pak@usz.ch*
1071-3581/$34.00

Abbreviations	
ACAOS	Anomalous coronary arteries originating from the opposite sinus of Valsalva
CCTA	Coronary computed tomography angiography
SPECT	Single photon emission computed tomography
MPI	Myocardial perfusion imaging
CAD	Coronary artery disease

INTRODUCTION

Anomalous coronary arteries originating from the opposite sinus of Valsalva (ACAOS) constitute one category among coronary artery anomalies and can be subdivided into anomalous origin of the right coronary artery (RCA) from the left coronary sinus (LCS), anomalous origin of the main stem, left anterior descending coronary artery (LAD) or left circumflex artery (LCX) from the right coronary sinus (RCS), and anomalous origin of the right or left coronary artery from the non-coronary sinus.[1-3] The incidence of ACAOS is reported to be around 1% in the general population.[4] ACAOS have been associated with angina pectoris, dyspnea, palpitations, ventricular arrhythmia, syncope, and sudden cardiac death (SCD).[5-10] The latter is particularly true for the so-called malignant variants of ACAOS, characterized by an interarterial course of the anomalous coronary artery between the aorta and pulmonary trunk (Figure 1). Malignant variants of ACAOS are considered to be the underlying cause of SCD in up to 20% in young athletes and up to 30% in military recruits.[11-13] The increased risk of SCD with this anomaly has been associated, apart from the interarterial course, with other anatomic high-risk features such as slit-like ostium, acute angle take-off, and intramural aortic segments.[13] Coronary computed tomography angiography (CCTA) is considered the primary imaging modality to detect and characterize the anatomy of ACAOS because it has a higher accuracy and detection rate than invasive coronary angiography, echocardiography, and magnetic resonance imaging.[14-16] Due to the increasing utilization of CCTA, increased absolute numbers of intentional and incidental diagnosis of coronary artery anomalies may be expected. However, there are no standardized guidelines for the workup of ACAOS detected by CCTA.[17] It remains unclear to what extent vessels with an anomalous course themselves may induce myocardial ischemia. Furthermore, discrimination between ACAOS and concomitant coronary artery disease (CAD)-related perfusion defects may be difficult. We hypothesized that hybrid imaging combining CCTA and single-photon emission computed tomography myocardial perfusion imaging (SPECT-MPI) may provide the means for such discrimination and offer an added value for risk stratification. The aim of the present study was to investigate the value of hybrid CCTA/SPECT-MPI in patients with ACAOS and possible concomitant CAD.

METHODS

Patient Population

We retrospectively identified patients with ACAOS revealed by CCTA who underwent additional clinically indicated SPECT-MPI at our institution between March 2003 and June 2015.

CCTA

CCTA was performed on multi-slice CT scanners (LightSpeed VCT XT, Discovery CT 750 HD, and Revolution CT, all GE Healthcare, Waukesha, WI, USA) according to current guidelines and as previously described.[18,19] Prior to examination, all patients received 2.5 mg isosorbiddinitrate sublingually (Isoket, Schwarz Pharma, Monheim, Germany) and up to 30 mg metoprolol (Beloc Zok, AstraZeneca, London, UK) was administered intravenously if the heart rate per minute was >65 in order to obtain optimal image quality.[19] Iodixanol (Visipaque 320, 320 mg·mL^{-1}, GE Healthcare) was injected into an antecubital vein followed by 50 mL saline solution. Volume and flow rate were adapted to body surface area.[20]

SPECT-MPI

All patients underwent a one-day 99m-Technetium-tetrofosmin stress/rest protocol according to the European procedural guidelines for radionuclide imaging of myocardial perfusion.[21] Briefly, physical stress testing was performed on a bicycle with a target heart rate of at least 85% of the predicted maximum age-corrected heart rate. Pharmacological stress was induced by adenosine (continuous infusion at 140 μg·kg^{-1}·minute^{-1}, with or without the combination of bicycle exercise) or dobutamine (incrementally infused, starting at 5 μg·kg^{-1}·minute^{-1} and increasing at 1-min intervals to a maximum of 60 μg·kg^{-1}·minute^{-1} until at least 85% of the predicted maximum heart rate had been reached). 99mTc-tetrofosmin was injected at peak physical or dobutamine stress or after 3 minutes of induced adenosine stress. Rest MPI was performed thereafter with the identical acquisition protocol after injection of a three times higher dose of 99mTc-tetrofosmin. Acquisition was performed either on a conventional standard dual-detector SPECT camera (Ventri, GE Healthcare) or on a novel gamma camera with cadmium-zinc-telluride (CZT) detector technology (Discovery NM 530c, GE Healthcare). Acquisition time on the conventional dual-head

SPECT camera was 15 minutes for stress and rest and 3 and 2 minutes for stress and rest, respectively, on the CZT camera.[22] A non-contrast-enhanced CT scan was performed for coronary artery calcium scoring (CACS) and attenuation correction of SPECT-MPI.[23] Calculation of CACS was performed in all patients, except in those with previous revascularization.

Coronary Anatomy

Coronary anatomic characteristics such as origin and course of ACAOS were recorded from volume-rendered images. Virtual angiographic view was used for evaluation of slit-like origin as a high-risk anatomic feature.[24,25] Double-oblique multiplanar reformatted images were used to identify other high-risk anatomic features such as take-off angle, intramural course and length, proximal and distal height/width vessel ratio, elliptical course (defined as height/width ratio of >1.3), proximal and distal vessel diameter area, and proximal vessel narrowing (Figure 2) of the anomalous vessels.[24,25] Coronary vessel dominance was classified as right dominant if the posterior descending artery and posterolateral branch originated from the RCA or as left dominant if originating from the LCX artery, and as balanced if the posterior descending artery originated from the RCA in combination with posterolateral branches originating from the LCX artery.[26] ACAOS with an interarterial course (between the aorta and pulmonary trunk) or a subpulmonary course (between the aorta and the right ventricular outflow tract) were classified as malignant, whereas all other variants were considered benign (Figure 1).[27] CAD was defined as a luminal diameter narrowing ≥50% as depicted by CCTA.

Hybrid Image Fusion

Datasets from SPECT-MPI and CCTA were fused on a dedicated workstation (Advantage Workstation 4.3, GE Healthcare) using a commercially available software tool (CardIQ Fusion, GE Healthcare) to create hybrid CCTA/SPECT-MPI images, as previously described in detail.[28] A matched CCTA/SPECT-MPI hybrid imaging finding was defined as a reversible (ischemia) or fixed (scar) SPECT-MPI defect in a territory subtended by an anomalous vessel or a stenotic coronary artery (defined as narrowing of the coronary luminal diameter ≥50%). All other combinations of pathologic findings were classified as unmatched.

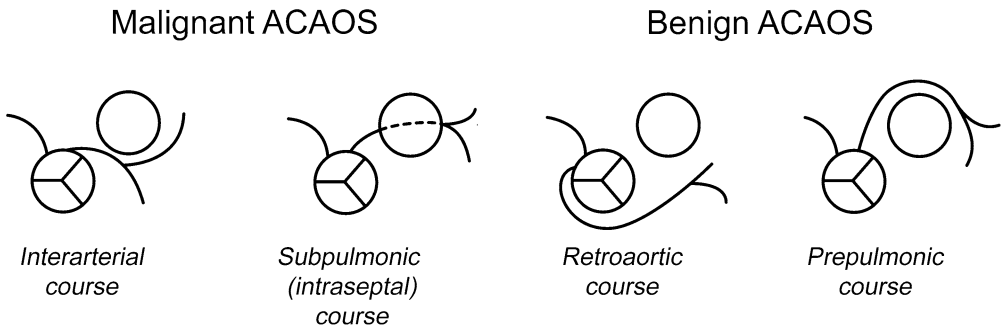

Figure 1. Schematic illustration of malignant and benign ACAOS variants according to the course of the anomalous coronary artery with respect to the aorta and the pulmonary trunk.

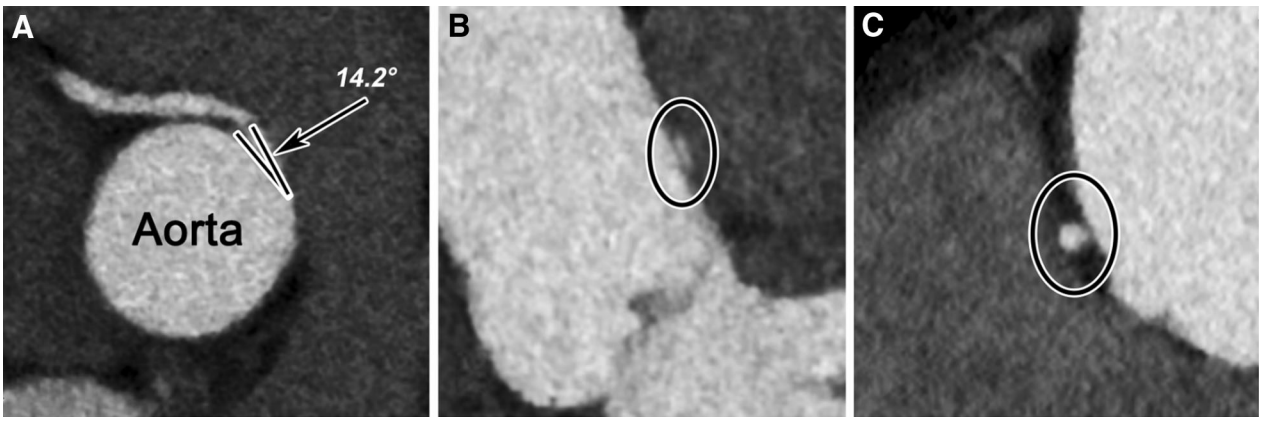

Figure 2. CCTA of a patient with malignant ACAOS variant and an RCA originating from LCS with an interarterial course. This anomaly shows high-risk anatomic features such as acute angle take-off (**A**), proximal intramural course with elliptic vessel shape, and high height/width ratio (**B**). By contrast, the distal vessel course shows a normal height/with ratio (**C**).

Statistical Analysis

All statistical analyses were performed using SPSS Statistics 22 (IBM Corporation, Armonk, NY). Data are reported as median ± interquartile range (IQR, 25th-75th percentile), or mean ± standard deviation (SD), or percentages for non-parametric and parametric data, respectively. Continuous variables were analysed using the Student's *t* test or Mann-Whitney *U* test, where appropriate. Categorical data were analyzed with Chi squared test or Fisheŕs exact test. A *P* value <.05 was considered statistically significant.

Ethics

This study conformed to the principles outlined in the declaration of Helsinki and was evaluated and approved by the local ethics committee, and the need for written informed consent was waived.

RESULTS

We identified 46 patients with ACAOS (mean age 56 ± 12 years, 80% male) who underwent both CCTA and SPECT-MPI. In 38 (82.6%) of the patients CCTA was followed by SPECT-MPI, whereas in the remaining eight patients SPECT-MPI was the first imaging modality. Table 1 depicts the types of ACAOS found. Patient characteristics are given in Table 2. Of note, CACS was significantly higher and patients with a history of CAD were significantly more frequent in the group of patients with benign ACAOS variants than in the group of patients with malignant ACAOS. An abnormal resting electrocardiogram was found in 8 (31%) of patients with a malignant and in 6 (30%) of patients with a benign ACAOS variant. During SPECT-MPI, 4 (15%) patients with a malignant ACAOS variant had an abnormal stress electrocardiogram and 4 (15%) complained of chest pain, compared to 2 (10%) and 3 (15%) of patients with a benign ACAOS variant, respectively (P = NS).

Of the 26 malignant ACAOS variants, 3 (11.5%) showed a subpulmonary course between the aorta and the right ventricular outflow tract, whereas the remaining 23 (88.5%) showed an interarterial course. Of the benign ACAOS variants, 1 (5%) showed a prepulmonary course, whereas the other 19 (95%) showed a retroaortic course (Figure 1).

Malignant ACAOS showed significantly more high-risk anatomic features such as slit-like ostium, acute angle take-off of the vessel, intramural course, higher proximal diameter ratio, and elliptical form of the proximal vessel (Table 3).

CCTA depicted obstructive CAD in 17 (40%) patients. SPECT-MPI revealed myocardial ischemia in 3.8% of patients with malignant ACAOS variants and in 30% ($P < .05$) of patients with benign ACAOS variants (Table 4). Vessel-based analysis using hybrid CCTA/SPECT-MPI revealed that ischemia was mainly due to obstructive CAD in a non-anomalous vessel (Figure 3). Two patients with a benign ACAOS variant (one LAD originating from the non-coronary sinus and one retroaortic course of an anomalous LCX) showed myocardial ischemia in the myocardial territory subtended by the anomalous vessel itself. However, in both patients, concomitant obstructive CAD (as diagnosed by CCTA) was also present in the anomalous coronary artery. Scars were present in 5 (19.2%) patients with malignant ACAOS and in 5 (25.0%) patients with benign ACAOS. Similarly, hybrid CCTA/SPECT-MPI showed that scars were due to CAD in non-anomalous vessels (Figure 4). Of note, in one patient with a malignant ACAOS variant, scar tissue could not be attributed to a coronary artery perfusion territory and was subsequently identified by cardiac magnetic resonance imaging as fibrosis due to myocarditis.

Five (10.9%) patients in whom relevant ischemia was detected by SPECT-MPI have undergone

Table 1. ACAOS characteristics

Characteristic	All, n = 46	Malignant, n = 26	Benign, n = 20
RCA originating from LCS, n (%)	23 (50.0%)	22 (84.6%)	1 (5.0%)
LCX originating from RCS, n (%)	15 (32.6%)	0	15 (75.0%)
Single right coronary artery, n (%)	4 (8.7%)	2 (7.7%)	2 (10.0%)
LM originating from non-coronary sinus, n (%)	2 (4.3%)	0	2 (10.0%)
LAD and LCX originating from RCS, n (%)	1 (2.2%)	1 (3.8%)	0
LAD originating from RCS, n (%)	1 (2.2%)	1 (3.8%)	0

RCA, Right coronary artery; *LCS*, left coronary sinus of Valsalva; *LCX*, left circumflex coronary artery; *RCS*, right coronary sinus of Valsalva; *LM*, left main stem; *LAD*, left anterior descending coronary artery.

Table 2. Patient characteristics

Characteristic	All, n = 46	Malignant, n = 26	Benign, n = 20	*P* value
Male gender, n (%)	37 (80%)	19 (73%)	18 (90%)	NS
Age (years), mean ± SD	56 ± 12	54 ± 12	59 ± 13	NS
Cardiovascular risk factors, n (%)				
Obesity (BMI > = 30 kg·m^{-2})	8 (17.4%)	4 (15.4%)	4 (20%)	NS
Smoking	16 (34.8%)	8 (30.8%)	8 (40.0%)	NS
Diabetes mellitus	4 (8.7%)	1 (3.8%)	3 (15.0%)	NS
Hypertension	9 (19.6%)	11 (42.3%)	11 (55.0%)	NS
Dyslipidemia	20 (43.5%)	8 (30.8%)	12 (60.0%)	.05
Positive family history	9 (19.6%)	4 (15.4%)	5 (25.0%)	NS
Known CAD, n (%)	19 (41.3%)	7 (26.9%)	12 (60.0%)	.020
History of revascularization, n (%)	6 (13.0%)	4 (15.4%)	2 (10.0%)	NS
Clinical symptoms, n (%)				
Asymptomatic	12 (26.1%)	6 (23.1%)	6 (30.0%)	NS
Typical angina pectoris	8 (17.4%)	6 (23.1%)	2 (10.0%)	NS
Atypical chest pain	14 (30.4%)	11 (42.3%)	3 (15.0%)	NS
Dyspnea	3 (6.5%)	0	3 (15.0%)	NS
Palpitations	6 (13.0%)	3 (11.5%)	3 (15.0%)	NS
Syncope	3 (6.5%)	0	3 (15.0%)	NS
CACS, median [IQR]	48 [0-300.0]	2 [0-143.5]	90 [38.3-387.0]	.010
Diagnostic test, n (%)				
Bicycle SPECT-MPI	14 (30.4%)	14 (53.8%)	0	<.001
Combined bicycle/adenosine SPECT-MPI	4 (8.7%)	2 (7.8%)	2 (10.0%)	NS
Dobutamine SPECT-MPI	5 (10.9%)	2 (7.7%)	3 (15.0%)	NS
Adenosine SPECT-MPI	23 (50.0%)	8 (30.8%)	15 (75.0%)	.007

CAD, Coronary artery disease; *SPECT-MPI*, single-photon emission computed tomography myocardial perfusion imaging; *SD*, standard deviation; *[IQR]*, interquartile range.

subsequent revascularization. No revascularization of anomalous vessels without CAD was performed.

DISCUSSION

Our results show that prevalence of CAD is relatively high in a middle-aged population of patients with coronary anomalies referred for non-invasive cardiac imaging due to suspected CAD. In these patients, the correct assignment of territories to the subtending coronary arteries may be particularly challenging. Even in patients with no coronary anomalies, the so-called standard distribution of myocardial perfusion territories does not correspond with individual anatomy in more than half of the patients.[29] Hybrid cardiac imaging fusing CCTA with SPECT-MPI has been introduced about one decade ago[28,30] and has been established as a tool for comprehensive anatomical and functional lesion evaluation[31,32] as well as for allocation of the affected coronary artery with the respective myocardial territory. Implementation of cardiac hybrid imaging may improve outcome prediction[33] and optimize downstream resource utilization.[34]

In our study, myocardial ischemia or scar was only found in patients who had concomitant obstructive CAD in the vessel matching the perfusion defect. It may be hypothesized that the anomalous course of the vessel per se may promote coronary insufficiency in coronary arteries additionally affected by CAD. However, the fact that most of the perfusion defects could be attributed to a myocardial territory subtended by a non-anomalous vessel with obstructive CAD or an anomalous vessel of benign variant but with concomitant obstructive CAD, with the absence of anatomic high-risk features, suggests that contribution of the anomaly itself may play only a minor role for the manifestation of myocardial perfusion deficits.

In line with the results of the present study, Uebleis et al demonstrated that out of 17 patients with ACAOS, one-third presented with myocardial ischemia in SPECT-MPI. However, only patients without concomitant CAD were included. Similar to our analysis, it could be shown that correlation between the anatomical variants of ACAOS and the presence of myocardial ischemia was low. Only in three patients perfusion defects could be matched to the territory of an

Table 3. Anatomic characteristics among malignant and benign ACAOS variants

Characteristic	Malignant, n = 26	Benign, n = 20	*P* value
Slit-like ostium, n (%)	18 (69.2%)	0	<.001
Intramural vessel course, n (%)	21 (80.8%)	2 (10.0%)	<.001
Intramural length (mm), median [IQR]	13.5 [10.0-15.3]	0	<.001
Acute take-off angle (<45%), n (%)	19 (73.1%)	7 (35.0%)	.010
Take-off angle (°), median [IQR]	23.0 [14.6-43.6]	66.4 [37.1-68.3]	.001
Proximal vessel diameter ratio (height/width), median [IQR]	2.2 [1.5-2.6]	1.3 [1.0-1.2]	<.001
Proximal diameter area (mm^2), median [IQR]	6.6 [5.4-10.5]	4.5 [4.7-11.9]	NS
Elliptic vessel course (proximal diameter ratio > 1.3), n (%)	22 (84.6%)	3 (15.0%)	<.001
Distal diameter ratio (height/width), median [IQR]	1.0 [1.0-1.1]	1.0 [1.0-1.1]	NS
Distal vessel diameter area (mm^2), median [IQR]	11.6 [9.4-14.2]	6.3 [5.0-9.7]	.001
Proximal vessel narrowing (%), median [IQR]	−37.0 [−50.9 to 9.5]	4.5 [−34.9 to 59.0]	.010
Coronary vessel dominance, n (%)			
Right vessel dominance	21 (80.8%)	17 (85.0%)	NS
Left vessel dominance	4 (15.4%)	1 (5.0%)	NS
Balanced vessel dominance	1 (3.9%)	2 (10.0%)	NS
Coronary vessel dominance supplied by anomalous vessel, n (%)	17 (65.4%)	3 (15.0%)	.001

[IQR], interquartile range.

Table 4. Perfusion defects in SPECT characterized by groups

Characteristic	Malignant, n = 26	Benign, n = 20	*P* value
Ischemia, n (%)	1 (3.8%)	6 (30.0%)	.033
Due to CAD, in a non-anomalous vessel	1 (3.8%)	4 (20.0%)	
Due to CAD, within an anomalous vessel	0	2 (10.0%)	
Scar, n (%)	5 (19.2)	5 (25.0%)	NS
Due to CAD, in a non-anomalous vessel	3 (11.5%)	4 (20.0%)	
Due to CAD, within an anomalous vessel	1 (3.8%)	1 (5.0%)	
Not matching the territory of a coronary vessel	1 (3.8%)	0	

CAD, Coronary artery disease.

anomalous vessel, and thereof two anomalies were malignant variants.[17] In accordance to previous studies, we found that malignant ACAOS had significantly more high-risk anatomic features such as slit-like ostium, intramural course, acute angle take-off of the vessel, higher proximal diameter ratio, and elliptical form of the proximal vessel compared to benign variants.[25,35] In contrast to our study, in a small population with malignant ACAOS revealed by invasive coronary angiography, De Luca et al demonstrated ischemia by SPECT-MPI in four out of five patients.[36] However, in this study it remained unclear whether myocardial ischemia or scar was matching the area of anomalous vessel perfusion.[29]

It is not known which study protocol is most adequate for the evaluation of myocardial perfusion in patients with ACAOS. This is to some extent reflected by the heterogeneous choice of stress testing protocols applied in the present study. In fact, bicycle exercise testing was performed in the majority of patients with a malignant variant of ACAOS, while in patients with a benign ACAOS variant stress was mostly induced pharmacologically. Dobutamine has been used in conjunction with intravascular ultrasound (IVUS) imaging

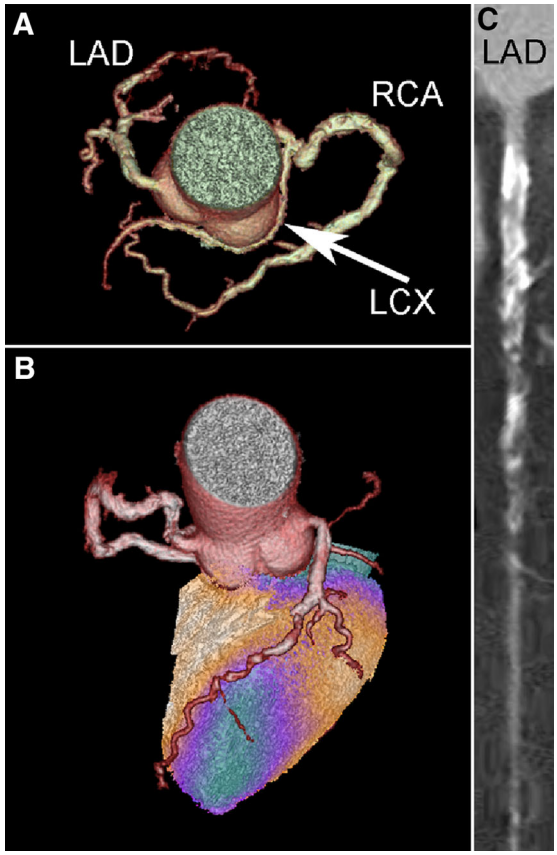

Figure 3. CCTA shows a patient with a benign ACAOS variant and a retroaortic course of the LCX (**A**). Hybrid CCTA/SPECT-MPI (using the CT attenuation-corrected stress dataset) reveals an anteroapical ischemia matching the perfusion area of the LAD (**B**). CCTA demonstrates severe coronary atherosclerosis with subtotal stenosis of the middle LAD (**C**).

in the assessment of ACAOS and demonstrated an anatomic compression of ovoid ostia in some patients as well as changes in the vessel diameter.[37] This suggests that dobutamine stress testing or bicycle exercise stress protocol might be preferable over adenosine, as this may most closely resemble the hemodynamic circumstances leading to dynamic vessel obstruction and potentially inducing myocardial ischemia during sports or daily physical activities.[36] However, Lim et al demonstrated that invasively measured fractional flow reserve in a malignant variant of ACAOS was similarly reduced by dobutamine and also adenosine. Therefore, adenosine might be an alternative option for functional evaluation of patients with ACAOS.[37] Furthermore, it remains uncertain whether standard physical stress protocols with a minimal heart rate of 85% of the predicted maximum heart rate is adequate, and it might be discussed whether more intense physical exertion beyond the level of established standard test protocols is needed in order to increase the detection rate of potential perfusion defects induced by ACAOS.

The present study extends our limited knowledge by demonstrating that in a middle-aged population significant impairment of myocardial perfusion due to the anomalous vessel in ACAOS per se is exceedingly rare and is much more likely attributable to concomitant CAD. Thus, hybrid imaging of CCTA/SPECT-MPI may offer a beneficial value for risk stratification of patients with either benign or malignant variants of ACAOS.

Whether coronary anomalies may constitute a co-factor promoting the incurrence of coronary

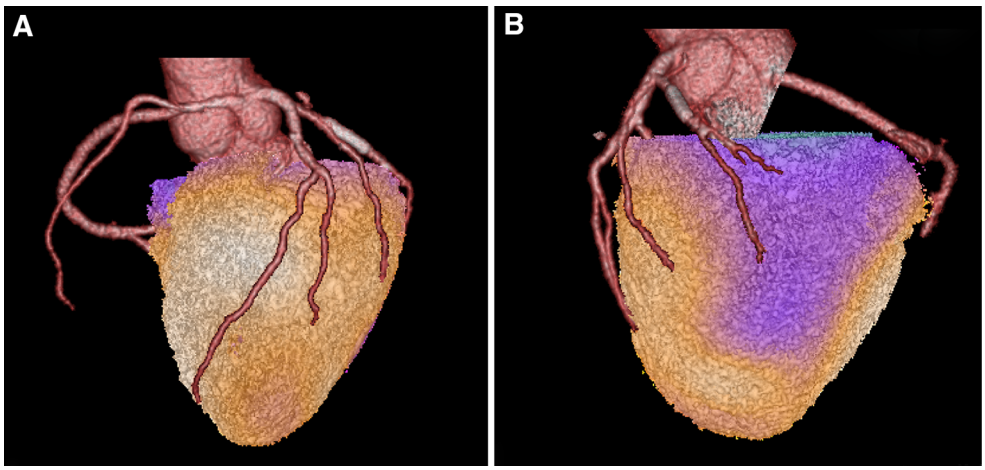

Figure 4. Hybrid CCTA/SPECT-MPI (using the CT attenuation-corrected rest dataset) shows a malignant ACAOS with the RCA originating from the LCS with an interarterial course. The inferolateral scar tissue could be clearly allocated to the perfusion territory subtended by the non-anomalous LCX which was previously revascularized with a stent due to occlusion and subsequent myocardial infarction (**A**, **B**).

insufficiency in case of concomitant coronary atherosclerosis remains yet to be elucidated.

LIMITATIONS

It may be perceived as a limitation that we retrospectively included patients referred for hybrid CCTA/SPECT-MPI as this may have led to a possible selection bias toward inclusion of patients with a higher prevalence of CAD. However, it has to be mentioned that 22% of the patients showed no calcifications. Older patients (over 30 years old) as represented in our population tend to have a decreased incidence of anomalous vessel-related sudden cardiac deaths and therefore possibly less anomalous vessel-related myocardial ischemia in SPECT-MPI.[38] Hence, extrapolation of our results for younger patients has to be made with caution.

NEW KNOWLEDGE GAINED

The present study shows the value of hybrid CCTA/SPECT-MPI in patients with ACAOS and possible concomitant CAD.

CONCLUSION

Hybrid CCTA/SPECT-MPI represents a valuable non-invasive tool to discriminate the impact of ACAOS from concomitant CAD on myocardial ischemia. The results of this study suggest that in a middle-aged population impairment of myocardial perfusion due to ACAOS per se may be exceedingly rare and is much more likely attributable to concomitant CAD.

Acknowledgments

We thank Verena Weichselbaumer, Edlira Loga, and Ennio Mueller for their excellent technical support.

Contributors

CG, DCB, CS, RRB, and PAK were responsible for the conception, design, analysis, and interpretation of the data and drafting of the manuscript. APP and OG were involved in the analysis and interpretation of the data and drafting of the manuscript. JV, FM, MP, OFC, JS, and TAF were involved in acquisition of data and drafting of the manuscript. All authors read and approved the final manuscript.

Disclosures

All authors have the following to disclose: The University Hospital of Zurich holds a research contract with GE Healthcare.

References

1. Angelini P. Coronary artery anomalies: An entity in search of an identity. Circulation 2007;115:1296-305.
2. Kim SY, Seo JB, Do K-HH, Heo J-NN, Lee JS, Song J-WW, et al. Coronary artery anomalies: Classification and ECG-gated multidetector row CT findings with angiographic correlation. Radiographics 2006;26:317.
3. Lim JC, Beale A, Ramcharitar S. Medscape. Anomalous origination of a coronary artery from the opposite sinus. Nat Rev Cardiol 2011;8:706-19.
4. Clark RA, Marler AT, Lin CK, McDonough RJ, Prentice RL, Malik JA, et al. A review of anomalous origination of a coronary artery from an opposite sinus of Valsalva (ACAOS) impact on major adverse cardiovascular events based on coronary computerized tomography angiography: A 6-year single center review. Ther Adv Cardiovasc Dis 2014;8:237-41.
5. Bria S, Chessa M, Abella R, Frigiola A, Bianco M, Palmieri V, et al. Aborted sudden death in a young football player due to anomalous origin of the left coronary artery: Successful surgical correction. J Cardiovasc Med (Hagerstown) 2008;9:834-8.
6. Camarda J, Berger S. Coronary artery abnormalities and sudden cardiac death. Pediatr Cardiol 2012;33:434-8.
7. Frommelt PC. Congenital coronary artery abnormalities predisposing to sudden cardiac death. Pacing Clin Electrophysiol 2009;32:S63-6.
8. Harmon KG, Drezner JA, Maleszewski JJ, Lopez-Anderson M, Owens D, Prutkin JM, et al. Pathogeneses of sudden cardiac death in national collegiate athletic association athletes. Circ Arrhythm Electrophysiol 2014;7:198-204.
9. Hill SF, Sheppard MN. A silent cause of sudden cardiac death especially in sport: Congenital coronary artery anomalies. Br J Sports Med 2014;48:1151-6.
10. Maron BJ, Doerer JJ, Haas TS, Tierney DM, Mueller FO. Sudden deaths in young competitive athletes: Analysis of 1866 deaths in the United States, 1980-2006. Circulation 2009;119:1085-92.
11. Basso C, Maron B, Corrado D, Thiene G. Clinical profile of congenital coronary artery anomalies with origin from the wrong aortic sinus leading to sudden death in young competitive athletes. J Am Coll Cardiol 1999;35:1493-501.
12. Eckart RE, Scoville SL, Campbell CL, Shry EA, Stajduhar KC, Potter RN, et al. Sudden death in young adults: A 25-year review of autopsies in military recruits. Ann Intern Med 2004;141:829-34.
13. Lorenz EC, Mookadam F, Mookadam M, Moustafa S, Zehr KJ. A systematic overview of anomalous coronary anatomy and an examination of the association with sudden cardiac death. Rev Cardiovasc Med 2006;7:205-13.
14. Datta J, White CS, Gilkeson RC, Meyer CA, Kansal S, Jani ML, et al. Anomalous coronary arteries in adults: Depiction at multidetector row CT angiography. Radiology 2005;235:812-8.
15. Ghadri JR, Kazakauskaite E, Braunschweig S, Burger IA, Frank M, Fiechter M, et al. Congenital coronary anomalies detected by coronary computed tomography compared to invasive coronary angiography. BMC Cardiovasc Disord 2014;14:81.
16. Schmid M, Achenbach S, Ludwig J, Baum U, Anders K, Pohle K, et al. Visualization of coronary artery anomalies by contrast-enhanced multi-detector row spiral computed tomography. Int J Cardiol 2006;111:430-5.
17. Uebleis C, Groebner M, von Ziegler F, Becker A, Rischpler C, Tegtmeyer R, et al. Combined anatomical and functional imaging using coronary CT angiography and myocardial perfusion SPECT

in symptomatic adults with abnormal origin of a coronary artery. Int J Cardiovasc Imaging 2012;28:1763-74.
18. Abbara S, Arbab-Zadeh A, Callister TQ, Desai MY, Mamuya W, Thomson L, et al. SCCT guidelines for performance of coronary computed tomographic angiography: A report of the Society of Cardiovascular Computed Tomography Guidelines Committee. J Cardiovasc Comput Tomogr 2009;3:190-204.
19. Buechel RR, Husmann L, Herzog BA, Pazhenkottil AP, Nkoulou R, Ghadri JR, et al. Low-dose computed tomography coronary angiography with prospective electrocardiogram triggering: Feasibility in a large population. J Am Coll Cardiol 2011;57:332-6.
20. Pazhenkottil AP, Husmann L, Buechel RR, Herzog BA, Nkoulou R, Burger IA, et al. Validation of a new contrast material protocol adapted to body surface area for optimized low-dose CT coronary angiography with prospective ECG-triggering. Int J Cardiovasc Imaging 2010;26:591-7.
21. Hesse B, Tägil K, Cuocolo A, Anagnostopoulos C, Bardiés M, Bax J, et al. EANM/ESC procedural guidelines for myocardial perfusion imaging in nuclear cardiology. Eur J Nucl Med Mol Imaging 2005;32:855-97.
22. Buechel RR, Herzog BA, Husmann L, Burger IA, Pazhenkottil AP, Treyer V, et al. Ultrafast nuclear myocardial perfusion imaging on a new gamma camera with semiconductor detector technique: First clinical validation. Eur J Nucl Med Mol Imaging 2010;37:773-8.
23. Schepis T, Gaemperli O, Koepfli P, Rüegg C, Burger C, Leschka S, et al. Use of coronary calcium score scans from stand-alone multislice computed tomography for attenuation correction of myocardial perfusion SPECT. Eur J Nucl Med Mol Imaging 2007;34:11-9.
24. Harris MA, Whitehead KK, Shin DC, Keller MS, Weinberg PM, Fogel MA. Identifying abnormal ostial morphology in anomalous aortic origin of a coronary artery. Ann Thorac Surg 2015;100:174-9.
25. Miller JA, Anavekar NS, El Yaman MM, Burkhart HM, Miller AJ, Julsrud PR. Computed tomographic angiography identification of intramural segments in anomalous coronary arteries with interarterial course. Int J Cardiovasc Imaging 2012;28:1525-32.
26. Gebhard C, Fuchs TA, Stehli J, Gransar H, Berman DS, Budoff MJ, et al. Coronary dominance and prognosis in patients undergoing coronary computed tomographic angiography: Results from the CONFIRM (COronary CT Angiography EvaluatioN For Clinical Outcomes: An InteRnational Multicenter) registry. Eur Heart J Cardiovasc Imaging 2015;16:853-62.
27. Sundaram B, Patel S, Bogot N, Kazerooni EA. Anatomy and terminology for the interpretation and reporting of cardiac MDCT: Part 1, Structured report, coronary calcium screening, and coronary artery anatomy. AJR Am J Roentgenol 2009;192:574-83.
28. Gaemperli O, Schepis T, Kalff V, Namdar M, Valenta I, Stefani L, et al. Validation of a new cardiac image fusion software for three-dimensional integration of myocardial perfusion SPECT and stand-alone 64-slice CT angiography. Eur J Nucl Med Mol Imaging 2007;34:1097-106.
29. Javadi MS, Lautamäki R, Merrill J, Voicu C, Epley W, McBride G, et al. Definition of vascular territories on myocardial perfusion images by integration with true coronary anatomy: A hybrid PET/CT analysis. J Nucl Med 2010;51:198-203.
30. Namdar M, Hany TF, Koepfli P, Siegrist PT, Burger C, Wyss CA, et al. Integrated PET/CT for the assessment of coronary artery disease: A feasibility study. J Nucl Med 2005;46:930-5.
31. Kajander S, Joutsiniemi E, Saraste M, Pietilä M, Ukkonen H, Saraste A, et al. Cardiac positron emission tomography/computed tomography imaging accurately detects anatomically and functionally significant coronary artery disease. Circulation 2010;122:603-13.
32. Rispler S, Keidar Z, Ghersin E, Roguin A, Soil A, Dragu R, et al. Integrated single-photon emission computed tomography and computed tomography coronary angiography for the assessment of hemodynamically significant coronary artery lesions. J Am Coll Cardiol 2007;49:1059-67.
33. Pazhenkottil AP, Nkoulou RNN, Ghadri J-RR, Herzog BA, Buechel RR, Küest SM, et al. Prognostic value of cardiac hybrid imaging integrating single-photon emission computed tomography with coronary computed tomography angiography. Eur Heart J 2011;32:1465-71.
34. Fiechter M, Ghadri JR, Wolfrum M, Kuest SM, Pazhenkottil AP, Nkoulou RN, et al. Downstream resource utilization following hybrid cardiac imaging with an integrated cadmium-zinc-telluride/64-slice CT device. Eur J Nucl Med Mol Imaging 2012;39:430-6.
35. Nasis A, Machado C, Cameron JD, Troupis JM, Meredith IT, Seneviratne SK. Anatomic characteristics and outcome of adults with coronary arteries arising from an anomalous location detected with coronary computed tomography angiography. Int J Cardiovasc Imaging 2015;31:181-91.
36. De Luca L, Bovenzi F, Rubini D, Niccoli-Asabella A, Rubini G, De Luca I. Stress-rest myocardial perfusion SPECT for functional assessment of coronary arteries with anomalous origin or course. J Nucl Med 2004;45:532-6.
37. Lim MJ, Forsberg MJ, Lee R, Kern MJ. Hemodynamic abnormalities across an anomalous left main coronary artery assessment: Evidence for a dynamic ostial obstruction. Catheter Cardiovasc Interv 2004;63:294-8.
38. Taylor AJ, Byers JP, Cheitlin MD, Virmani R. Anomalous right or left coronary artery from the contralateral coronary sinus: ''High-risk'' abnormalities in the initial coronary artery course and heterogeneous clinical outcomes. Am Heart J 1997;133:428-35.